ACS APPLIED MATERIALS & INTERFACES

RESEARCH ARTICLE

www.acsami.org

Anatase TiO_2 Crystal Facet Growth: Mechanistic Role of Hydrofluoric Acid and Photoelectrocatalytic Activity

Haimin Zhang,[†] Yun Wang,[†] Porun Liu,[†] Yanhe Han,[†] Xiangdong Yao,[‡] Jin Zou,[§] Huiming Cheng,[⊥] and Huijun Zhao*[,†]

[†]Centre for Clean Environment and Energy, and Griffith School of Environment, Griffith University, Gold Coast Campus, QLD 4222, Australia

[‡]QLD Micro- and Nanotechnology Centre, Griffith University, Nathan Campus, QLD 4111, Australia

[§]Materials Engineering and Centre for Microscopy and Microanalysis, University of Queensland, QLD 4072, Australia

[⊥]Shenyang National Laboratory for Materials Science, Institute of Metal Research, Chinese Academy of Science, Shenyang 110016, China

Supporting Information

ABSTRACT: This work reports a facile hydrothermal approach to directly grow anatase TiO_2 crystals with exposed {001} facets on titanium foil substrate by controlling pH of HF solution. The mechanistic role of HF for control growth of the crystal facet of anatase TiO_2 crystals has been investigated. The results demonstrate that controlling solution pH controls the extent of surface fluorination of anatase TiO_2, hence the size, shape, morphology, and {001} faceted surface area of TiO_2 crystals. The theoretical calculations reveal that {001} faceted surface fluorination of anatase TiO_2 can merely occur via dissociative adsorption of HF molecules under acidic conditions while the adsorption of Na^+F^- is thermodynamically prohibited. This confirms that the presence of molecular form of HF but not F^- is essential for preservation of exposed {001} facets of anatase TiO_2. Anatase TiO_2 crystals with exposed {001} facets can be directly fabricated on titanium foil by controlling the solution pH ≤ 5.8. When pH is increased to near neutral and beyond (e.g., pH ≥ 6.6), the insufficient concentration of HF ([HF] ≤ 0.04%) dramatically reduces the extent of surface fluorination, leading to the formation of anatase TiO_2 crystals with {101} facets and titanate nanorods/nanosheets. The anatase TiO_2 nanocrystals with exposed {001} facets exhibits a superior photoelectrocatalytic activity toward water oxidation. The findings of this work clarify the mechanistic role of HF for controlling the crystal facet growth, providing a facile means for massive production of desired nanostructures with high reactive facets on solid substrates for other metal oxides.

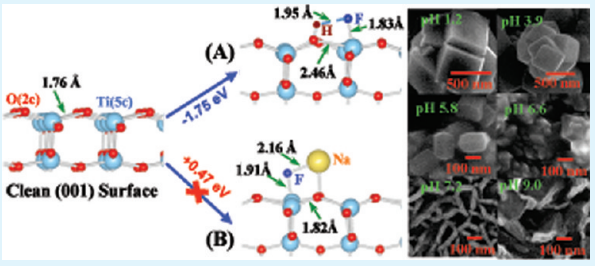

KEYWORDS: anatase TiO_2, microspheres, nanocrystals, {001} facets, photoelectrocatalysis

1. INTRODUCTION

Superior properties of anatase TiO_2 crystals with exposed {001} facets make it a promising material for applications such as environmental remediation and energy conversion.[1−12] Although {001} faceted crystal surfaces are preferred, the as-synthesized anatase crystals are usually dominated by the energetically favored {101} faceted surfaces (0.44 J/m^2).[13,14] {001} faceted surfaces having a relatively higher surface energy (0.90 J/m^2) compared to other anatase TiO_2 crystal facets can be readily diminished during the crystal growth process.[13,14] A recently reported new synthetic approach have demonstrated that high {001} faceted surface energy status can be effectively reduced by surface fluorination, enabling the growth of anatase crystals with 47% of exposed {001} facets.[1] Much effort has since been dedicated to fabricate anatase TiO_2 with high percentage of exposed {001} facets.[2,4−6] All experimental data and theoretical calculation results reported to date have indicated that a fluorine rich crystal surface is essential for preservation of {001} facets during crystal growth.[1−5] It has also been suggested that proper fluorine rich crystal surface environment can only be attained under acidic conditions.[1−5] This implies that pH of the reaction medium plays a critical role in determining the surface fluorination, thus the size of exposed {001} facets of anatase TiO_2. As a weak acid, HF solution speciation (HF molecules and F^-) is determined by pH. The initial adsorption step taking place at the {001} faceted surface could be strongly affected by the solution species (e.g., HF or F^-), determining the adsorption pathway and amount. Although significant role of surface fluorination for preservation of {001} faceted surfaces has been reported,[1] the mechanistic aspects, especially the preferential adsorption species (e.g., HF or F^-) on {001} faceted surfaces, and the relationship between adsorption amount and surface area of exposed {001} facets remain elusive. To this end, development of a facile approach enabling controllable growth of anatase TiO_2

Received: March 23, 2011
Accepted: May 25, 2011
Published: May 25, 2011

 © 2011 American Chemical Society

crystals with desirable morphologies and exposed {001} facets by controlling the solution species (via pH control), and further revealing the mechanistic role of HF for the {001} crystal facet growth would be useful to guide further research in the field. In addition, it has been well documented that immobilizing TiO_2 onto solid conducting substrates is essential for almost all applications involving electrochemistry or photoelectrocatalysis.[15−17] To better serve such needs, it is critical to develop a synthetic approach capable of directly growing anatase TiO_2 crystals with exposed {001} facets onto a conductive substrate.

Here we report for the first time a one-pot facile hydrothermal approach to directly grow anatase TiO_2 crystals onto a titanium foil substrate with controllable morphology and size of exposed {001} facets, in which the metal titanium foils are employed not only as the conductive substrate but also responsible to supply the required titanium sources for the crystal growth. A key strategy of this approach is to control pH of the reaction medium to achieve a controlled growth of morphology and size of anatase TiO_2 crystals with exposed {001} facets. The mechanistic role of reaction solution pH affecting structure, morphology and formation of exposed {001} faceted anatase TiO_2 crystals were investigated in detail based on experimental data and theoretical calculations. The photocatalytic activity of the resultant nanostructured photoanodes consisting of anatase TiO_2 crystals with exposed {001} reactive facets were evaluated for photoelectrocatalytic water oxidation.[18,19]

2. EXPERIMENTAL SECTION

2.1. Chemicals and Materials. Titanium (Ti) foils (0.25 mm thick, 99.7% purity) were supplied by Aldrich Corporation. Hydrofluoric acid (HF, 48%), acetone, 2-propanol, and methanol (analytical grade) were purchased from Sigma-Aldrich without further treatment prior to use. High-purity deionized water (Millipore Corp., 18 MΩ cm) was used for the electrolyte solution preparation and the rinse of Ti substrates.

2.2. Synthesis. Titanium foils (50 mm ×15 mm ×0.25 mm) were degreased prior to experiments by sonication in acetone, 2-propanol, and methanol, subsequently rinsed with Milli-Q water, and finally dried in a nitrogen stream.[20] The pretreated titanium foil as substrate was placed in an autoclave and 60 mL of 0.5% (v/v) HF solution with different pHs was added to the autoclave. The hydrothermal reaction was carried out at 180 °C for 3 h. After hydrothermal reaction, the obtained samples were rinsed with Milli-Q water and dried in a N_2 stream. To obtain a clean fluorine-free surface, the resultant samples were calcined in air at 600 °C for 1.5 h with heating and cooling rates of 2°/min. The TiO_2 nanoparticulate film photoanode was fabricated with dip-coating method by sol−gel technique.[21] The coated photoanodes were calcined in a muffle furnace at 450 °C for 2 h in air with heating and cooling rates of 2 °C/min.

2.3. Characterization. The synthesized products were comprehensively characterized by SEM (JSM-6300F), TEM (Philips F20), XRD (Shimadzu XRD-6000 diffractometer), and XPS (Kratos Axis ULTRA incorporating a 165 mm hemispherical electron energy analyzer). All binding energies were carefully aligned by referenced to the C 1s peak (285.0 eV) arising from surface hydrocarbons or possible adventitious hydrocarbon.

2.4. Theoretical Calculations. All density functional theory (DFT) computations were performed using the Quantum Espresso (QE) package.[22] Electron-ion interactions were described using the Vanderbilt-type ultrasoft pseudopotentials.[23] A plane-wave basis set was employed with a kinetic energy cutoff of 30 Ry. For the electron−electron exchange and correlation interactions, the functional of Perdew, Burke and Ernzerhof (PBE),[24] a form of the general gradient approximation (GGA), were used throughout. The anatase TiO_2 surface was modeled by a supercell comprising a six-layer slab separated by a vacuum region of 10 Å. When the geometry was optimized, the top four atomic layers and the adsorbates were allowed to relax, while the lower two layers were fixed at the ideal bulk-like position. We perform Brillouin-zone integrations using Monkhorst-Pack grids of special points. (1 × 2 × 1) *k*-points meshes were employed for the (001) (4 × 2) surface cell for the calculations of adsorption energies, which included eight Ti atoms and 16 oxygen atoms each atomic layer. The *k*-points meshes in our calculation have been demonstrated in the previous calculations.[25]

2.5. Photoelectrochemical Measurements. The photoelectrochemical measurements were performed at 23 °C in a photoelectrochemical cell with a quartz window for illumination.[26] It consisted of a TiO_2 photoanode, a saturated Ag/AgCl reference electrode, and a platinum mesh counter electrode. A voltammograph (CV-27, BAS) was used for the application of potential bias. Potential and current signals were recorded using a Macintosh (AD Instruments). The illuminated area of the photoanode was 0.785 cm^2. A 0.10 M $NaNO_3$ solution was used as the electrolyte. Illumination was carried out using a 150 W xenon arc lamp light source with focusing lenses (HF-200W-95, Beijing Optical Instruments). To avoid the electrolyte being heated-up by the infrared light, a UV-band-pass filter (UG 5, Avotronics Pty. Ltd.) was used. The light intensity was regulated and carefully measured at 365 nm.

3. RESULTS AND DISCUSSION

3.1. Structural and Morphological Properties. In this work, the hydrothermal reaction was performed at 180 °C for 3 h in 0.5% (v/v) HF solution with different pHs. The crystallographic structure of the as-synthesized samples has been confirmed by X-ray diffraction (XRD, Cu Kα radiation) as shown in Figure 1. It was found that the as-synthesized products obtained from the reaction solution pH ≤ 5.8 are tetragonal anatase TiO_2 with a space group of $I4_1/amd$ (JCPDS No. 21−1272).[2] Figure 2 shows SEM and TEM images of the as-synthesized anatase TiO_2 products under different pHs (pH 1.2, 3.9, and 5.8). When pH was controlled at 1.2, TiO_2 microspheres with a mean size of 2.1 μm were obtained (Figure 2a). The surface of these microspheres was covered by square-shaped crystals, having an average area of 0.46 μm^2 exposed plane crystal facets, as shown in the inset in Figure 2a. TEM was employed to study detail structural characteristics of the anatase TiO_2 sample (Figure 2b). The corresponding SAED pattern (top inset in Figure 2b) confirms that the square-shaped plane facet is a single crystal, the zone axis is [001], hence the faceted surface is the (001) surface.[1,2,8,9,27] The HRTEM image (bottom inset in Figure 2b) shows a perpendicular lattice spacing of 0.19 nm, representing the (200) and (020) atomic planes of the anatase TiO_2, further confirms the exposed crystal facet is the {001} facet.[1,2,8,9,27] When pH was set at 3.9, the average size of the randomly packed microspheres was reduced to 1.0 μm (Figure 2c). High magnification SEM image (Inset in Figure 2c) reveals a surface covered by square-shaped crystals having a mean planar facet area of 0.11 μm^2. TEM image, and corresponding SAED pattern and HRTEM image confirm that the plane facets are the {001} faceted surfaces (Figure 2d). It should be noted that the above SAED and HRTEM data were obtained from the microsphere samples after ultrasonic treatment.[8,9,27] Interestingly, with pH 5.8, TiO_2 microspheres disappeared and the dispersive TiO_2 nanocrystals with a truncated tetragonal bipyramidal shape were formed (Figure 2e). The mean planar facet area was found to be 0.02 μm^2. SAED and

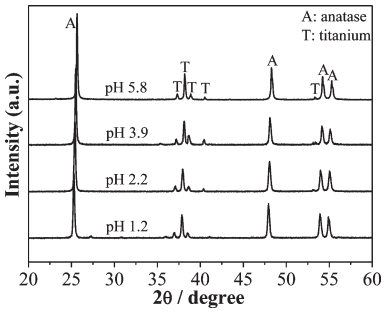

Figure 1. XRD patterns of as-synthesized TiO_2 samples obtained at 180 °C for 3 h in 0.5% (v/v) HF solutions with different pH values (pH 1.2, 2.2, 3.9, and 5.8).

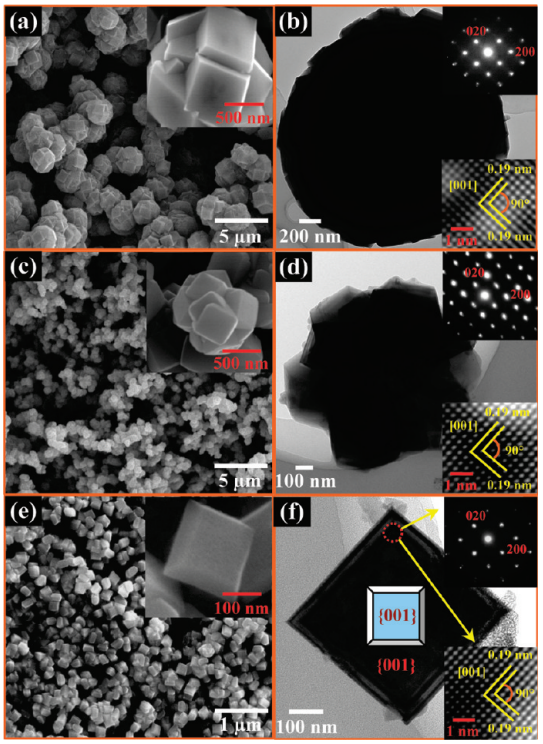

Figure 2. SEM and TEM images of as-synthesized TiO_2 samples obtained at different pH solutions. The insets in a, c, and e correspond to high-magnification SEM images; the insets in b, d, and f correspond to SAED patterns (top) and HRTEM images (bottom). Middle inset in f is a {001}-projected geometrical model of the anatase nanocrystal. (a, b) pH 1.2; (c, d) pH 3.9; and (e, f) pH 5.8.

HRTEM data confirm that the top/bottom square-shaped plane facets are {001} facets and the eight isosceles trapezoidal facets are {101} facets (Figure 2f).[1,2] Under the experimental conditions employed, anatase TiO_2 crystals with different morphologies and exposed {001} facets can be obtained in HF solutions with pH ≤ 5.8.

The effect of further increasing solution pH (pH > 5.8) on the morphologies and crystalline structures of the resultant products was also investigated. Figure 3 shows typical SEM images of the as-synthesized products obtained from reaction solutions pH > 5.8. Figure 3a shows the SEM image of the as-synthesized product from a reaction solution with pH 6.6. The obtained particulate morphology differs remarkably from the dispersive truncated tetragonal bipyramidal shaped TiO_2 nanocrystals with

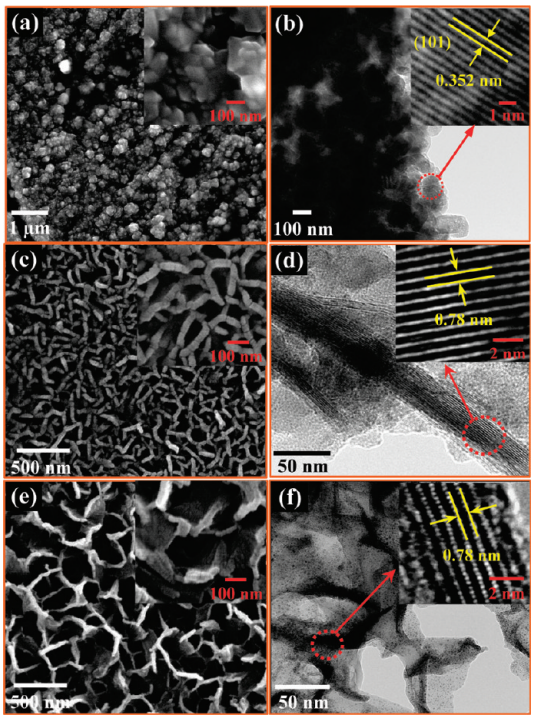

Figure 3. SEM images of the as-synthesized products obtained at 180 °C for 3 h in HF reaction solutions with pH > 5.8. The insets in a, c, and e correspond to high magnification SEM images; the insets in b, d, and f correspond to HRTEM images. (a, b) pH 6.6; (c, d) pH 7.2; and (e, f) pH 9.0. The measured interlayer spacing was found to be 0.78 nm in the insets in d and f and can be assigned to titanate nanostructures.[29,30]

exposed {001} facets obtained from pH 5.8 reaction solution. HRTEM data reveal a fringe spacing of 0.352 nm, corresponding to the (101) planes of anatase TiO_2 (Figure 3b).[28] In other words, {101} faceted surface dominated anatase TiO_2 crystals were obtained when pH was increased to 6.6, confirming that a pH change can lead to a crystal facet change. When pH >7.0, titanate nanorods and nanosheets were obtained as evidenced by SEM and TEM analyses (Figure 3c–f), demonstrating that a further increase in the reaction solution pH can lead to a crystal phase change.[29,30] The results shown in Figures 2 and 3 demonstrate that the pH of the reaction medium can be used to control the crystal growth not only on morphological and dimensional parameters but also crystal phases and crystal facets, as summarized in Table 1.

3.2. Surface Fluorination and {001} Faceted Planar Area. It has been well-documented that the amount of TiO_2 surface bonded-fluorine depends strongly on solution pH.[31,32] X-ray photoelectron spectra (XPS) of as-synthesized TiO_2 samples were first investigated. Figure 4a shows a representative XPS spectrum taken from TiO_2 nanocrystals obtained at pH 5.8. The spectrum shows the peak of F 1s as well as those of Ti, O, and C elements. Similar XPS spectra with varied intensities of F 1s peaks can be obtained from all samples investigated. Figure 4b shows the high-resolution XPS spectra of F 1s. F 1s peak centered at ca. 685.0 eV is clearly visible for all samples.[31,33] The relative intensity of F 1s spectra decreased with increased pH, indicating a decrease in the amount of the surface-bonded fluorine that agrees with the reports by Choi et al., where they found that an acidic medium is favorable for the formation of TiO_2 surface-bonded fluorine and the TiO_2 surface fluorination barely occurs in

Table 1. Effect of Hydrothermal Reaction Conditions on Morphological, Dimensional and Crystal Phase of As-Synthesized Products

reaction conditions	morphology of nanostructures	average Size (μm)	average {001} facets Size (μm)	$S_{\{001\}}$ (μm^2)
pH 1.2, 0.5% (v/v) HF, 180 °C for 3 h	anatase TiO_2 microspheres with exposed {001} facets	2.1 ± 0.08	0.680 ± 0.030	0.4624 ± 0.0350
pH 2.2, 0.5% (v/v) HF, 180 °C for 3 h	anatase TiO_2 microspheres with exposed {001} facets	1.5 ± 0.05	0.544 ± 0.025	0.2959 ± 0.0130
pH 3.9, 0.5% (v/v) HF, 180 °C for 3 h	anatase TiO_2 microspheres with exposed {001} facets	1.0 ± 0.03	0.329 ± 0.016	0.1082 ± 0.0060
pH 5.8, 0.5% (v/v) HF, 180 °C for 3 h	anatase TiO_2 nanocrystals with exposed {001} facets	0.19 ± 0.01	0.133 ± 0.007	0.01769 ± 0.00050
pH 6.6, 0.5% (v/v) HF, 180 °C for 3 h	anatase TiO_2 nanocrystals with exposed{101} facets	0.090 ± 0.004	———	———
pH 7.2, 0.5% (v/v) HF, 180 °C for 3 h	titanate nanorods	0.030 ± 0.001	———	———
pH 9.0, 0.5% (v/v) HF, 180 °C for 3 h	titanate nanosheets	0.010 ± 0.0007	———	———

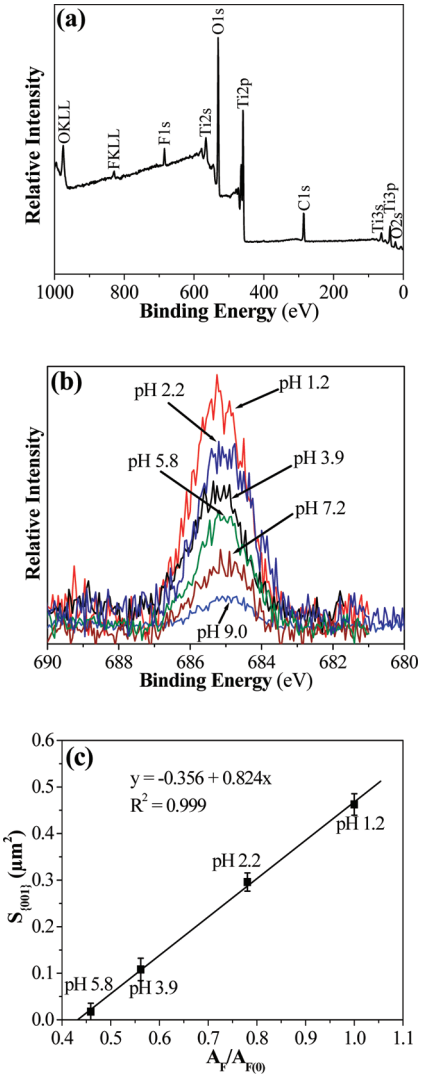

Figure 4. (a) Representative XPS survey spectra of anatase TiO_2 nanocrystals with exposed {001} facets on titanium foil substrate obtained at pH 5.8. (b) High-resolution XPS spectra of F 1s of as-synthesized TiO_2 samples obtained at different pH solutions. (c) Relationship of $A_F/A_{F(0)}$ and $S_{\{001\}}$.

alkaline medium.[31,32] The relative amount of TiO_2 surface-bonded fluorine can be estimated from the fitted peak area (denoted as A_F) of the F 1s XPS spectra.[34] To quantify the relationship between solution pH and {001} facets growth of anatase TiO_2 crystals (for the samples obtained in HF solutions with pH $\leq$5.8), the average {001} faceted planar area (denoted as $S_{\{001\}}$, and estimated in term of square[2]) and corresponding A_F values were carefully measured. Figure 4c shows the plot of $A_F/A_{F(0)}$ (where $A_{F(0)}$ represents the fitted peak area of F 1s at pH 1.2) against $S_{\{001\}}$. A surprisingly well-defined linear relationship (R^2 = 0.999) was obtained. Data shown in Figure 4c also alludes to that the {001} faceted planar surface area would approach to zero ({001} facets can no longer be preserved) when the surface-bonded fluorine was reduced to a critical value (i.e., $A_F/A_{F(0)} \leq 0.432$, or $A_F \leq 1249$ in our case), which is corresponding to pH > 5.8. Considering {101} facets dominated TiO_2 nanocrystals (Figure 3a,b) obtained at pH 6.6, and a further increase in solution pH will lead to the formation of titanate nanorods/nanosheets (Figure 3c–f), it can be concluded that the amount of surface-bonded fluorine becomes insufficient for {001} facets preservation in a nearly neutral medium. The above results demonstrate that solution pH determines the amount of surface-bonded fluorine, hence the {001} faceted planar surface area. Given the critical role of solution pH played, scientific insight of fundamental steps involved in surface fluorination processes is extremely important and deserves a further investigation.

3.3. Mechanistic Role of Hydrofluoric Acid. To understand the effect of solution pH on {001} facets growth of anatase TiO_2, the first principle density functional theory (DFT) was used to calculate the reaction energies of the adsorption of the dominant adsorbent (via pH control) on (001) surface of anatase TiO_2. In this work, the possible adsorption species could include HF, F^-, H^+ and Na^+ (Na^+ originated from NaOH for solution pH adjustment). Owing to the strong H–F bonding energy (D_0 = 5.91 eV),[35] HF is a weak acid (pK_a = 3.17), which means that the HF molecules and Na^+F^- will be the dominant species at low and high pHs, respectively (see Figure S1 in the Supporting Information). The adsorption of HF or Na^+F^- on the anatase TiO_2 (001) surface is therefore considered in DFT calculations to simulate the situations in the acidic or nearly neutral medium, respectively (Figure 5). The strength of HF or Na^+F^- interacting with (001) surface was reflected by their adsorption energy (ΔE), which is calculated according to the following equation:

$$\Delta E = E_{tot} - E_{surf} - E_{ad}$$

where E_{tot} and E_{surf} are the optimized total energies of systems with and without adsorbent, respectively, E_{ad} represents the energy of the optimized isolated HF or the energy per Na^+F^- of the bulk crystal.

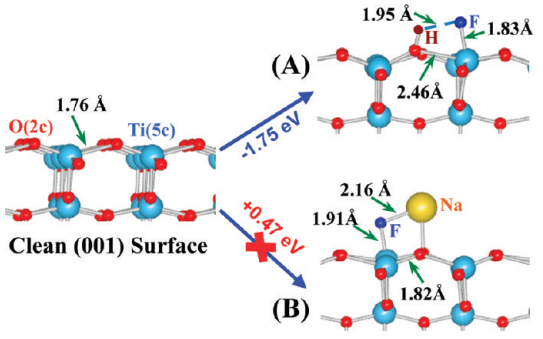

Figure 5. Top view of HF/Na^+F^- on an anatase TiO_2 (001) surface with the (8 × 4) surface cell. (A) the adsorption of HF; (B) the adsorption of Na^+F^-.

DFT calculations confirm that under acidic conditions, the dissociative adsorption of HF molecules on {001} faceted crystal surfaces is energetically permitted as demonstrated by the strong adsorption energy of −1.75 eV (Figure 5A). In strong contrast, the interaction of Na^+F^- with {001} faceted crystal surfaces is thermodynamically prohibited as shown by the calculated adsorption energy of +0.47 eV (Figure 5B). The differences for HF and Na^+F^- adsorption on {001} faceted surfaces of anatase TiO_2 can be attributed to the different bonding energies for O−H and O−Na. The bonding energy of O−H (−4.43 eV) is almost 1.7 times of that for O−Na (−2.65 eV),[35] favorable for the dissociative adsorption of molecular form of HF on {001} faceted surfaces. The strongly adsorbed HF on (001) surface dramatically increases the length of surrounding Ti−O from 1.76 Å to 2.46 Å (see the Supporting Information for details). In addition, the DFT calculations also demonstrate that the dissociative adsorption of HF molecules can effectively reduce the {001} faceted anatase TiO_2 surface energy to −0.50 J/m^2, which is obviously lower than the clean (001) surface energy of 0.90 J/m^2 and the (101) surface energy of 0.44 J/m^2 (see Supporting Information for details).[24] This confirms that the surface fluorination *via* dissociative adsorption of HF facilitates the growth of {001} facets and stabilizes the grown {001} facets.

The above demonstrated pH controlled growth can be attributed to two types of HF involvements in the structural formation processes. On one hand, HF plays a key role as a dissolution reagent, providing basic building materials for structural formation.[10] On the other hand, HF serves as a facet controlling reagent, facilitating the growth of {001} faceted surface and stabilizing the grown {001} facets.[1,2] Regarding the effect of solution pH on HF role as a dissolution reagent, under hydrothermal conditions, a high acidity (low pH, e.g., pH 1.2) leads to a rapid dissolution of titanium substrate producing H_2TiF_6.[10] The produced H_2TiF_6 reacts with H_2O to form randomly oriented TiO_2 seeds, which are subsequently aggregated to form the cores that are further developed into TiO_2 microspheres. At low pHs, the surface fluorination via dissociative adsorption of HF makes the [001] direction a preferential crystal growth direction due to the reduced {001} faceted surface energy.[1,2,28] This leads to the formation of TiO_2 microsphere having protrusive square-shaped surface structures with exposed plane {001} facets or truncated tetragonal bipyramidal shaped TiO_2 nanocrystals with exposed {001} facets.[1,9] Under such circumstances, the control of the reaction solution pH essentially controls the solution speciation. A fluorinated crystal surface with reduced surface energy facilitates the growth of {001} facets and preserves the grown {001} facets. The DFT calculations confirmed that the {001} faceted surface fluorination can occur only through dissociative adsorption of molecular form of HF under acidic conditions, while the {001} faceted surface fluorination via adsorption of Na^+F^- (in near neutral and basic reaction media) is thermodynamically prohibited. The size of {001} facets of anatase TiO_2 crystals depends on the extent of surface fluorination, which is closely related to the effective concentration of molecular form HF in reaction solution that is determined by pH of the reaction solution. This gives a rise to control the size of exposed {001} facets by controlling the pH. When pH > 5.8, the HF induced dissolution process slows, leading to a slow structural formation process. In near neutral and basic reaction media (e.g., pH ≥ 6.6), the insufficient concentration of molecular form HF ([HF] ≤ 0.04%, see Figure S1 in Supporting Information) dramatically reduces the extent of surface fluorination, leading to the formation of low surface energy {101} facets dominated anatase TiO_2 and titanate nanorods/nanosheets. In other word, the presence of molecular form of HF but not F^- is essential for preservation of exposed {001} facets of anatase TiO_2.

3.4. Photoelectrocatalytic Activity. The superior photocatalytic activity of anatase TiO_2 crystals with exposed {001} facets has been previously reported.[1,2] However, the photoelectrocatalytic activity of anatase TiO_2 crystals with exposed {001} facets have not yet been reported. In this study, water was chosen as a probe compound to evaluate the photoelectrocatalytic activity due to the global interest in TiO_2 photocatalysis-based water splitting technique for hydrogen production.[17,36] Prior to the measurements, all photoanodes fabricated by directly grown anatase TiO_2 nanostructures with exposed {001} facets on the titanium foil substrates were subjected to a calcination treatment at 600 °C for 1.5 h in air to remove the surface-bonded fluorine without altering the as-synthesized nanostructures.[2,4] Figure S2a (see the Supporting Information) shows a SEM image of TiO_2 nanocrystal photoanode (obtained at pH 5.8 as an example) after calcination. No noticeable change in morphology was observed, indicating high thermal stability of TiO_2 nanocrystals with exposed {001} facets.[2,4] Similar results were obtained for anatase TiO_2 microspheres fabricated at other pH solutions. XRD investigation also suggests no phase transformation taken place during calcination for anatase TiO_2 nanocrystal photoanode (obtained at pH 5.8, see Figure S2b in Supporting Information).[2,4] Similar results were also obtained for anatase TiO_2 microsphere products fabricated at other pH solutions. For comparison, anatase TiO_2 nanoparticulate film photoanode was also prepared. Figure S3 (see the Supporting Information) shows typical SEM image and XRD pattern of the TiO_2 nanoparticulate film photoanode after calcination at 450 °C for 2 h. XRD pattern (see Figure S3a in the Supporting Information), SAED pattern (inset in Figure S3b, Supporting Information), and SEM image (Figure S3b, Supporting Information) demonstrated that the fabricated TiO_2 nanoparticulates were anatase without exposed {001} facets. All photoanodes were then sealed into a specially designed electrode holder with a defined area of 0.785 cm^2 left open for UV illumination.[18,19,37] It should be noted that the TiO_2 microsphere sample obtained at pH 1.2 cannot be used as photoanode for photoelectrocatalytic experiment because of almost dissolved titanium foil after 3 h of reaction in strong acidic solution.

Figure 6a shows the voltammograms of water oxidation at a set of photoanodes made of truncated tetragonal bipyramidal shaped TiO_2 nanocrystals (pH 5.8) or TiO_2 microspheres (pH

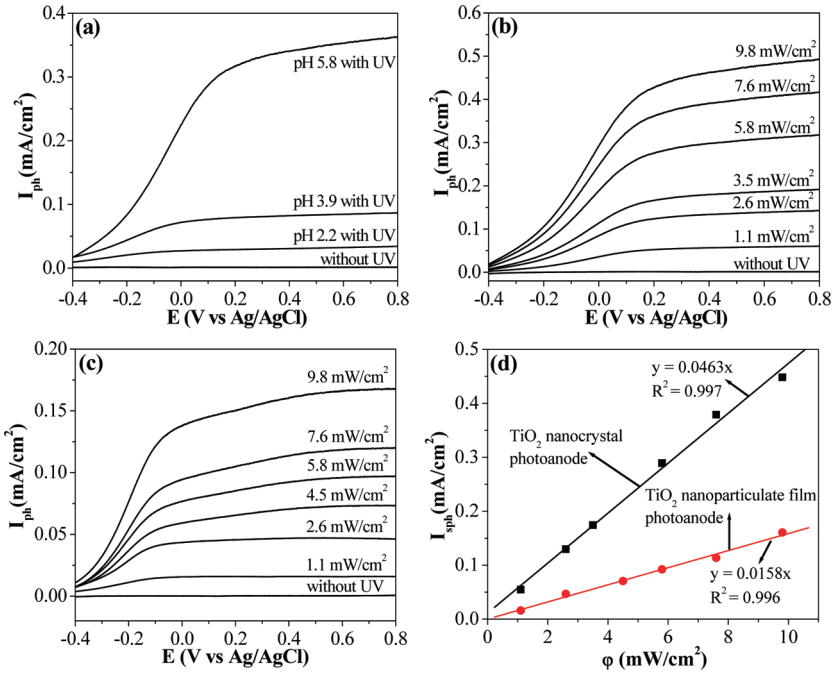

Figure 6. (a) Voltammograms of TiO_2 nanostructured photoanodes synthesized at different pH solutions obtained from 0.10 M $NaNO_3$ electrolyte. Scan rate = 5.0 mV/s and light intensity = 6.6 mW/cm^2. (b) Voltammograms of anatase TiO_2 nanocrystal photoanode synthesized at pH 5.8 obtained in 0.10 M $NaNO_3$ electrolyte at different light intensity. (c) Voltammograms of anatase TiO_2 nanoparticulate film photoanode synthesized by sol−gel method obtained in 0.10 M $NaNO_3$ electrolyte at different light intensity. (d) The relationship of saturation photocurrents for two TiO_2 nanostructured photoanodes and light intensity. The saturation photocurrents for two TiO_2 nanostructured photoanodes measured at +0.4 V and derived from b and c, respectively.

2.2 and pH 3.9) with exposed {001} facets in 0.10 M $NaNO_3$ electrolyte, with or without UV illumination. It can be seen that without UV illumination, no measurable photocurrent was observed. Under UV illumination, all photoanodes investigated exhibit the identical I_{ph}−E characteristics. In all cases, the photocurrent increased linearly with applied potential bias within the lower potential range because the overall photocatalytic process was limited by the photoelectron transport inside the photocatalyst layer.[18,37] The photocurrent saturated at higher potentials can be attributed to the limitation of the photohole generation/capture processes at TiO_2 surface.[18,19,26,37] Under such conditions, the measured saturation photocurrent (I_{sph}) represents the maximum rate of photoelectrocatalytic oxidation of water.[18,19,26,38] Among all photoanodes, the highest photoactivity toward water oxidation was obtained from the photoanode fabricated by the dispersive anatase TiO_2 nanocrystals obtained at pH 5.8. The photoelectrocatalytic activity of the anatase TiO_2 microspheres was found to be directly related to the size of the microspheres. An increase in the microsphere size leads to a decrease in the photoelectrocatalytic activity. Although the larger size microspheres possess larger {001} faceted planar area, the markedly reduced overall effective surface area with increased microsphere sizes overpower the positive effect contributed by the increased {001} faceted surface area, leading to a decreased photocatalytic activity. The photoelectrocatalytic activity of the dispersive anatase TiO_2 nanocrystal photoanode was subsequently compared with that of the anatase TiO_2 nanoparticulate film photoanode. Panels b and c in Figures 6 show the voltammograms of the two nanostructured photoanodes in a 0.10 M $NaNO_3$ electrolyte, with or without UV illumination. I_{sph} values under different light intensities were derived from voltammograms shown in panels b and c in Figure 6 at +0.40 V, and plotted the UV light intensities, φ (Figure 6d). Linear relationships were obtained for both photoanodes shown slope values of 0.0463 mA/mW (R^2 = 0.997) and 0.0158 mA/mW (R^2 = 0.996) for the nanocrystal and nanoparticulate film photoanodes, respectively. For a given set of experimental conditions, the slope of the $I_{sph}-\varphi$ curve quantitatively represents the photoelectrocatalytic activity of the photoanode. Figure 6d revealed that the slope obtained from the dispersive anatase TiO_2 nanocrystals with exposed {001} facets (1.2 μm in thickness) was nearly 3 times of that for the anatase TiO_2 nanoparticulate film photoanode (1.0 μm in thickness), confirming a significantly improved photoelectrocatalytic activity of the dispersive anatase TiO_2 nanocrystal photoanode. Considering the lower density of the {001} faceted dispersive TiO_2 nanocrystal photoanode (Figure 2e) in comparison with the anatase TiO_2 nanoparticulate film photoanode (see Figure S3b in the Supporting Information), it is reasonable to attribute such a significantly improved photoelectrocatalytic activity to the dispersive {001} faceted anatase TiO_2 nanocrystal photoanode.[39]

4. CONCLUSION

In summary, we have demonstrated that under hydrothermal conditions and in presence of HF, the controlled growth of TiO_2 crystals with different size, morphology, crystal phase and facet can be achieved by simply controlling the pH of the reaction media. Anatase TiO_2 crystals with exposed {001} facets can be directly fabricated on titanium foil substrate by controlling the reaction media pH ≤5.8. DFT calculations have confirmed that the {001} faceted anatase TiO_2 surface fluorination can occur only through dissociative adsorption of molecular form HF under acidic conditions, whereas the surface fluorination adsorption of

Na^+F^- is thermodynamically prohibited. This confirms that the presence of molecular form of HF but not F^- is essential for preservation of exposed {001} facets of anatase TiO_2. A fluorinated crystal surface with reduced surface energy facilitates the growth of {001} facets and preserves the grown {001} facets. The extent of the surface fluorination strongly depends on the concentration of HF molecules that determines the size, shape, morphology, and the {001} faceted planar surface area of the resultant anatase TiO_2 crystals. The fabricated anatase TiO_2 nanocrystals with exposed {001} facets demonstrated a significantly improved photoelectrocatalytic activity toward water oxidation, confirming the superiority of the {001} faceted anatase crystal surfaces for photocatalysis and photoelectrocatalysis based applications. The findings of this work clarify the mechanistic role of HF for controlling the crystal facet growth, providing a facile means for massive production of desired nanostructures with high reactive facets on solid substrates for other metal oxides.

■ ASSOCIATED CONTENT

Supporting Information. Details of theoretical calculations, solution species distribution, XRD pattern and SEM image of calcined nanocrystal sample, and XRD pattern and SEM image of calcined nanoparticulate sample. This material is available free of charge via the Internet at http://pubs.acs.org/.

■ AUTHOR INFORMATION

Corresponding Author
*E-mail: h.zhao@griffith.edu.au. Tel: 61-7 55528261. Fax: 61-7 55528067.

■ ACKNOWLEDGMENT

This work was financially supported by Australian Research Council. This research was undertaken on the NCI National Facility in Canberra, Australia, which was supported by the Australian Commonwealth Government.

■ REFERENCES

(1) Yang, H. G.; Sun, C. H.; Qiao, S. Z.; Zou, J.; Liu, G.; Smith, S. C.; Cheng, H. M.; Lu, G. Q. *Nature* **2008**, *453*, 638.
(2) Yang, H. G.; Liu, G.; Qiao, S. Z.; Sun, C. H.; Jin, Y. G.; Smith, S. C.; Zou, J.; Cheng, H. M.; Lu, G. Q. *J. Am. Chem. Soc.* **2009**, *131*, 4078.
(3) Liu, G.; Yang, H. G.; Wang, X.; Cheng, L.; Pan, J.; Lu, G. Q.; Cheng, H.-M. *J. Am. Chem. Soc.* **2009**, *131*, 12868.
(4) Zhang, D.; Li, G.; Yang, X.; Yu, J. C. *Chem. Commun.* **2009**, 4381.
(5) Han, X.; Kuang, Q.; Jin, M.; Xie, Z.; Zheng, L. *J. Am. Chem. Soc.* **2009**, *131*, 3152.
(6) Chen, J. S.; Tan, Y. L.; Li, C. M.; Cheah, Y. L.; Luan, D.; Madhavi, S.; Boey, F. Y. C.; Archer, L. A.; Lou, X. W. *J. Am. Chem. Soc.* **2010**, *132*, 6124.
(7) Yu, J.; Qi, L.; Jaroniec, M. *J. Phys. Chem. C* **2010**, *114*, 13118.
(8) Zhang, H.; Han, Y.; Liu, X.; Liu, P.; Yu, H.; Zhang, S.; Yao, X.; Zhao, H. *Chem. Commun.* **2010**, *46*, 8395.
(9) Liu, M.; Piao, L.; Lu, W.; Ju, S.; Zhao, L.; Zhou, C.; Li, H.; Wang, W. *Nanoscale* **2010**, *2*, 1115.
(10) Wu, G.; Wang, J.; Thomas, D. F.; Chen, A. *Langmuir* **2008**, *24*, 3503.
(11) Alivov, Y.; Fan, Z. Y. *J. Phys. Chem. C* **2009**, *113*, 12954.
(12) Liu, S.; Yu, J.; Jaroniec, M. *J. Am. Chem. Soc.* **2010**, *132*, 11914.
(13) Diebold, U. *Surf. Sci. Rep.* **2003**, *48*, 53.
(14) Yin, Y.; Alivisatos, A. P. *Nature* **2005**, *437*, 664.
(15) Kim, D.; Ghicov, A.; Albu, S. P.; Schmuki, P. *J. Am. Chem. Soc.* **2008**, *130*, 16454.
(16) Gratzel, M. *Nature* **2001**, *414*, 338.
(17) Mor, G. K.; Shankar, K.; Paulose, M.; Varghese, O. K.; Grimes, C. A. *Nano Lett.* **2005**, *5*, 191.
(18) Jiang, D.; Zhao, H.; Zhang, S.; John, R. *J. Phys. Chem. B* **2003**, *107*, 12774.
(19) Zhang, H.; Zhao, H.; Zhang, S.; Quan, X. *ChemPhysChem* **2008**, *9*, 117.
(20) Macak, J. M.; Tsuchiya, H.; Taveira, L.; Aldabergerova, S.; Schmuki, P. *Angew. Chem., Int. Ed.* **2005**, *44*, 7463.
(21) Nazeeruddin, M. K.; Kay, A.; Rodicio, I.; Humphry-Baker, R.; Mueller, E.; Liska, P.; Vlachopoulos, N.; Graetzel, M. *J. Am. Chem. Soc.* **1993**, *115*, 6382.
(22) Giannozzi, P.; Baroni, S.; Bonini, N.; Calandra, M.; Car, R.; Cavazzoni, C.; Ceresoli, D.; Chiarotti, G. L.; Cococcioni, M.; Dabo, I.; Dal Corso, A.; de Gironcoli, S.; Fabris, S.; Fratesi, G.; Gebauer, R.; Gerstmann, U.; Gougoussis, C.; Kokalj, A.; Lazzeri, M.; Martin-Samos, L.; Marzari, N.; Mauri, F.; Mazzarello, R.; Paolini, S.; Pasquarello, A.; Paulatto, L.; Sbraccia, C.; Scandolo, S.; Sclauzero, G.; Seitsonen, A. P.; Smogunov, A.; Umari, P.; Wentzcovitch, R. M. *J. Phys.-Condes. Matter* **2009**, *21*, 95502.
(23) Vanderbilt, D. *Phys. Rev. B* **1990**, *41*, 7892.
(24) Perdew, J. P.; Burke, K.; Ernzerhof, M. *Phys. Rev. Lett.* **1996**, *77*, 3865.
(25) Lazzeri, M.; Vittadini, A.; Selloni, A. *Phys. Rev. B: Condens. Matter Mater. Phys.* **2001**, *63*, 155409/1.
(26) Zhang, H.; Liu, P.; Liu, X.; Zhang, S.; Yao, X.; An, T.; Amal, R.; Zhao, H. *Langmuir* **2010**, *26*, 11226.
(27) Hu, X.; Zhang, T.; Jin, Z.; Huang, S.; Fang, M.; Wu, Y.; Zhang, L. *Cryst. Growth Des.* **2009**, *9*, 2324.
(28) Zhou, J. K.; Lv, L.; Yu, J.; Li, H. L.; Guo, P.-Z.; Sun, H.; Zhao, X. S. *J. Phys. Chem. C* **2008**, *112*, 5316.
(29) Yuan, Z.-Y.; Su, B.-L. *Colloids Surf., A* **2004**, *241*, 173.
(30) Stengl, V.; Bakardjieva, S.; Subrt, J.; Vecernikova, E.; Szatmary, L.; Klementova, M.; Balek, V. *Appl. Catal., B* **2006**, *63*, 20.
(31) Park, H.; Choi, W. *J. Phys. Chem. B* **2004**, *108*, 4086.
(32) Vohra, M. S.; Kim, S.; Choi, W. *J. Photochem. Photobiol., A* **2003**, *160*, 55.
(33) Pan, J. H.; Zhang, X.; Du, A. J.; Sun, D. D.; Leckie, J. O. *J. Am. Chem. Soc.* **2008**, *130*, 11256.
(34) Wang, Q.; Chen, C.; Zhao, D.; Ma, W.; Zhao, J. *Langmuir* **2008**, *24*, 7338.
(35) *Handbook of Chemistry and Physics*, 81st ed.; Lide, D. R., Ed.; CRC Press: Boca Raton, FL, 2000.
(36) Mor, G. K.; Varghese, O. K.; Wilke, R. H. T.; Sharma, S.; Shankar, K.; Latempa, T. J.; Choi, K.-S.; Grimes, C. A. *Nano Lett.* **2008**, *8*, 1906.
(37) Jiang, D.; Zhao, H.; Zhang, S.; John, R. *J. Catal.* **2004**, *223*, 212.
(38) Jiang, D.; Zhang, S.; Zhao, H. *Environ. Sci. Technol.* **2007**, *41*, 303.
(39) Tachikawa, T.; Yamashita, S.; Majima, T. *J. Am. Chem. Soc.* **2011**, *133*, 7197.